engineering proceedings

MDPI

Proceeding Paper

CAD Representation of the Mullins Effect from the SEGE 80 Flexible Coupling Model †

Stefan Tenev [1,*], Ismail Mehmedov [2], Aleksandrina Bankova [2], Nina Nedeva [2], Stefan Stefanov [2], Rosen Hristov [2], Asparuh Atanasov [2], Plamen Nikolov [2] and Svetoslav Petrov [2]

[1] Faculty of Manufacturing and Technologies, Mechanics and Mechanical Elements, University of Varna, 9000 Varna, Bulgaria
[2] Department of Mechanics and Mechanical Elements, University of Varna, 9000 Varna, Bulgaria; imehmedov.me@abv.bg (I.M.); ina_janakiewa@abv.bg (A.B.); ninanedeva@tu-varna.bg (N.N.); stefanov_48@abv.bg (S.S.); rosen.hristov@tu-varna.bg (R.H.); info@1art.eu (A.A.); plam_07@abv.bg (P.N.); svetoslavp1988@gmail.com (S.P.)
* Correspondence: stefo_83@tu-varna.bg; Tel.: +359-887015142
† Presented at the International Conference on Electronics, Engineering Physics and Earth Science (EEPES'24), Kavala, Greece, 19–21 June 2024.

Abstract: A Mullins simulation was conducted to analyze the effects of loading and unloading of a flexible-type SEGE coupling with a nominal torque of $T_{nom} = 80$ Nm and maximum torque of $T_{max} = 120$ Nm. The coupling's properties were determined by examining its moment characteristics at $T = 120,\ 100,\ 80,\ 60,\ 40,$ and 20 Nm. The correlation between the Mullins effect results obtained from the SEGE coupling load simulation via SolidWorks 2022 software and the actual experimental data was examined.

Keywords: Mullins effect; simulation; computer model; flexible; coupling

1. Introduction

The Mullins effect is a mechanical response observed in highly elastic "Rubber" type materials where the stress–strain curve is conditioned upon the pre-applied maximum load [1–5]. This phenomenon leads to an immediate increase in the elasticity (softening) of the material, which occurs when the load surpasses a previous maximum value. Conversely, when the load is below the previous maximum, nonlinear elastic behavior is displayed.

A comparative analysis of the Mullins effect was undertaken in a static study [6] of a flexible SEGE 80 coupling (Figure 1), standardized according to BDS 16420-86 [7]. The study includes simulations in the SolidWorks 2022 CAD system, involving the application of a load to that coupling [8–13]. The working elements of the coupling are rubber cylinders, position 2, compressed by thumbs evenly distributed at 360° across the front surfaces of the two semi-couplings—position 1 and 3. The cylinder press is carried out by rotating one semi-coupling on its axis relative to the other semi-coupling, which is fixed. Due to the viscoelastic properties of the "Rubber", a "Generalized Maxwell model" is utilized in the simulation software system to calculate the deformation state of the material, specifically for the working cylinders of the coupling [14–18].

check for updates

Citation: Tenev, S.; Mehmedov, I.; Bankova, A.; Nedeva, N.; Stefanov, S.; Hristov, R.; Atanasov, A.; Nikolov, P.; Petrov, S. CAD Representation of the Mullins Effect from the SEGE 80 Flexible Coupling Model. *Eng. Proc.* **2024**, *70*, 22. https://doi.org/10.3390/engproc2024070022

Academic Editor: Grigor Mihaylov

Published: 2 August 2024

Copyright: © 2024 by the authors. Licensee MDPI, Basel, Switzerland. This article is an open access article distributed under the terms and conditions of the Creative Commons Attribution (CC BY) license (https://creativecommons.org/licenses/by/4.0/).

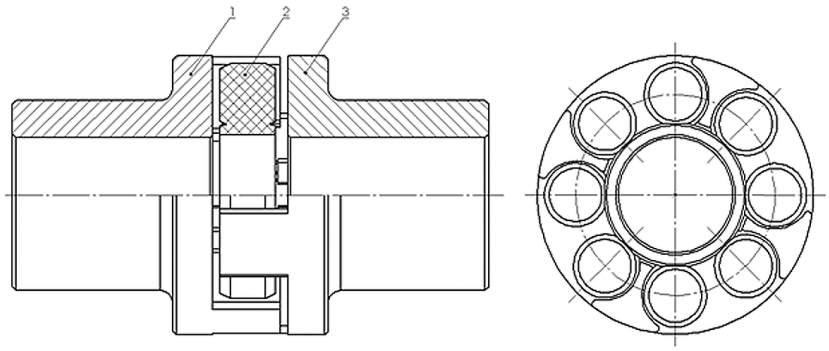


Figure 1. Flexible-type SEGE 80 coupling.

2. Exposition

The Mullins effect is a phenomenon that describes the "softening" of rubbers during the initial maximum deformation. This significant alteration in the mechanical properties of rubbers following the first elongation results in residual deformation and induced anisotropy. To represent the Mullins effect, the performance of the SEGE 80 coupling was tested, for the scope of the present research, in accordance with a program that aligns with the methodology described in the regulatory document BDS 16638-87 [7].

Experimental studies were conducted to evaluate the damping capabilities of the coupling using torque values measured at $T = 120,\ 100,\ 80,\ 60,\ 40$ and 20 Nm [6], with a maximum load at $T_{max} = 120$ Nm. The results of these studies are graphically visualized in Figure 2, with the dashed line representing the coupling unloadings.

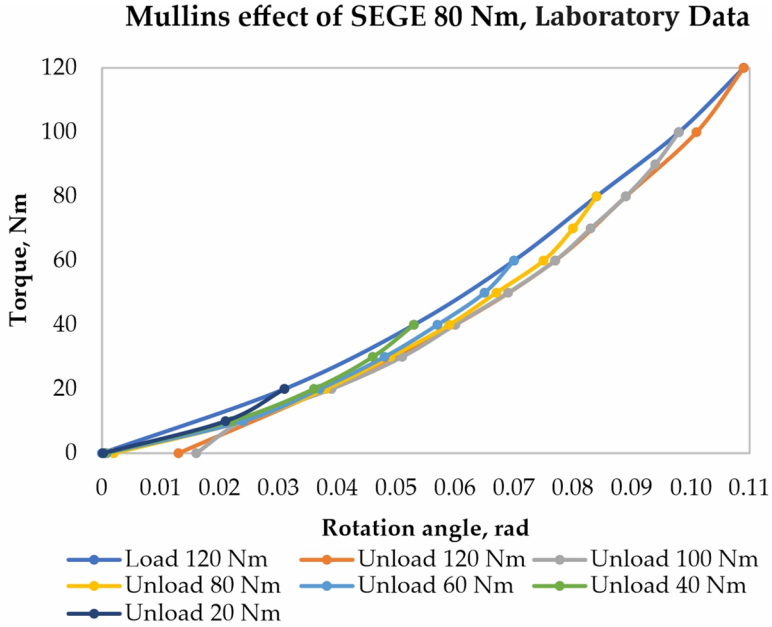


Figure 2. Experimental study of the SEGE 80 coupling in terms of the damping capability of the Mullins effect.

A computer model was created based on the design of the flexible coupling, with the material of the working cylinders pre-set as "viscoelastic" and mechanical property values closely resembling those in the "Generalized Maxwell model" (Table 1) [19].

The computer model of the SEGE 80 coupling was developed to meet the dimensions specified in BDS 16420-86 [7]. The working surfaces within the coupling consist of the concave cylindrical surface of the floated semi-coupling thumb (Figure 3, position 1), concave cylindrical surface of the fixed semi-coupling thumb (Figure 3, position 3) and the cylindrical surface of the rubber cylinder (Figure 3, position 2). Through torque from the

floated semi-coupling, the thumb "position 1" compresses the cylinder "position 2" on the fixed thumb "position 3".

Table 1. Mechanical characteristics and parameters required for viscoelastic material simulation.

Model Type—Viscoelastic					
№	Parameter	Symbol	Value	Unit of measurement	Commentary
1.	Elastic Modulus	E	11	MPa	Modulus of linear deformation
2.	Poisson's Ration	υ	0.49	-	Poisson ratio
3.	Shear Modulus	G	3.69	MPa	Modulus of angular deformation
4.	Thermal Expansion Coefficient	T	0.0002	K^{-1}	Coefficient of thermal expansion for "EPDM" rubber
5.	Tensile Strength	S_{eH}	17	MPa	Tensile strength
6.	Shear Relaxation Modulus (1)	g	0.45		Modulus of relaxation (0–1, 1—maximum energy absorption)
7.	Time Values (Shear Relaxation Modulus 1)	t	1	s	Range of relaxation time
8.	Glassy Transition Temperature	Tg	−55/218.15	C/K	Glass transition temperature
9.	Mass Density	r	1430	kg/m^3	Density of "EPDM" rubber
Nonliner Static Properties					
	Stepping options				Settings of the simulation steps
1.	Start time		0	s	Start time of the simulation
2.	End time		20	s	End time of the simulation
	Time increment (autostepping)				Settings of the simulation step time
1.	Initial time increment		0.2		Initial time increment
2.	Min		0		Minimum step time
3.	Max		20		Maximum step time
4.	No. of adjustments		5		Number of adjustments
	Geometry nonlinearity options				Occurrences of geometric nonlinearity
	Use large displacement formulation		yes		Computations in the event of large displacements
	Large strain option		yes		Computations in the event of large relative deformations
	Solver				Method of solution
	Automatic Solver Selection		yes		Automatic method for obtaining a solution
	Incompatible bonding options				Options with incompatible bonding
	Simplified		yes		Simplified bonding
	Step/Tolerance options				Step/Tolerance
1.	Do equilibrium iteration every		1 step (s)		Using iterations to achieve system equilibrium for each step
2.	Maximum equilibrium iterations		20		Maximum number of iterations to achieve equilibrium
3.	Convergence tolerance		0.01		Relative displacement tolerance used to achieve system equilibrium convergence
4.	Maximum incremental strain		0.1		Maximum increase in relative strain
5.	Singularity elimination factor (0–1)		0		Uncertainty factor

The working cylindrical surfaces of the coupling have parallel axes and varying radius values. The binding between these surfaces is, theoretically, expected to be in a "line", presupposing, in turn, the impact of contact stress experienced by the working elements. To prevent potential errors in the tolerance conditions of the coupling load simulation, a sufficiently small contact area is modeled on the working cylindrical surfaces (Figure 4) [20].

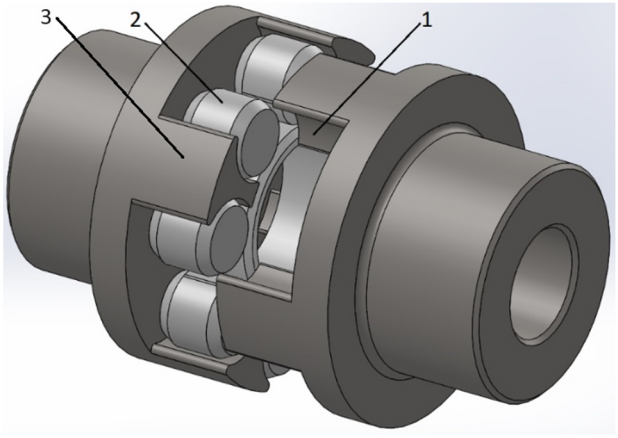


Figure 3. Elastic-type SEGE 80 coupling.

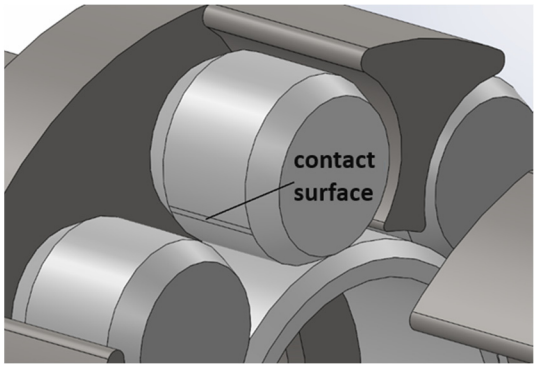


Figure 4. Contact surface on the working cylindrical surfaces.

The SEGE 80 coupling simulation is conducted with a prior maximum torque of $T_{max} = 120$ Nm. The strain distribution pattern for the rubber coupling element is illustrated in Figure 5.

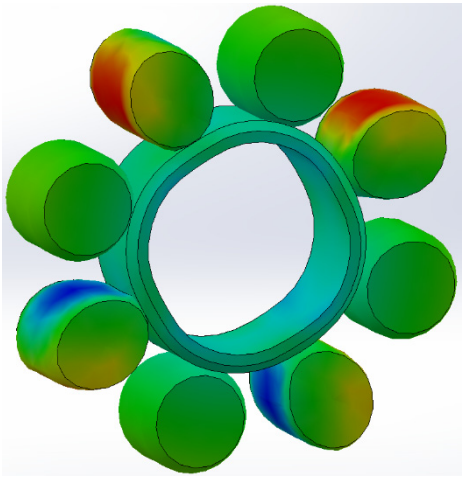


Figure 5. Rubber element deformation of SEGE 80 coupling with $T_{max} = 120$ Nm.

3. Results and Discussion

To adhere to the theoretical model of the Mullins effect, the unloading of the three-dimensional model was carried out sequentially with torque values of $T = 120$, 100, 80, 60, 40 and 20 Nm [6]. The simulation data were analyzed and are graphically represented in Figure 6.

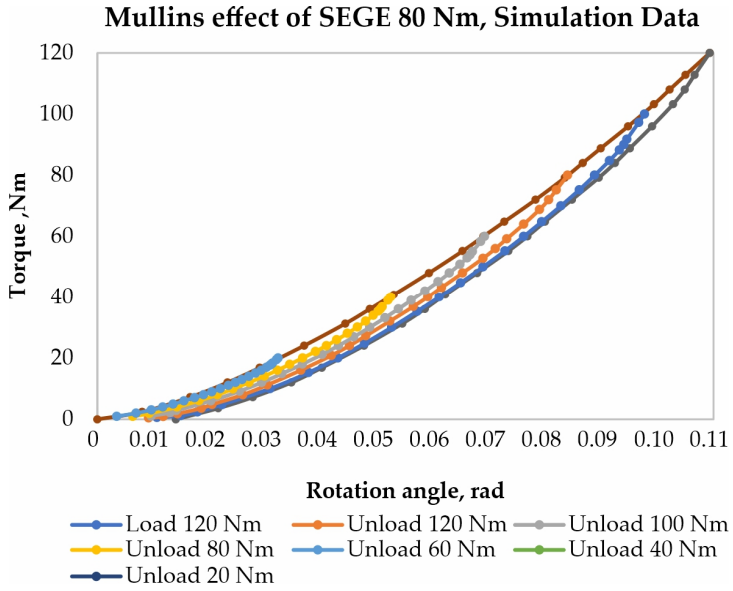


Figure 6. Simulation study of the SEGE 80 coupling in terms of the damping capability of the Mullins effect.

The foundation of this study was taken from [19], but, due to the additional results of the Mullins effect, this research is more precise in terms of the concepts used.

4. Conclusions

This article describes a methodology for studying the SEGE coupling, in which a comparative analysis is made between a laboratory study and a software simulation to examine the damping capability of the Mullins effect. The aim of the analysis is to prepare a theoretical model of the coupling, sufficiently close to the experimental one, with a percentage difference of the Mullins effect in both models of up to 2.5%. This accurate theoretical model can be used for the geometry optimization of rubber elements and semi-couplings, which can improve the overall performance of the coupling without the need for a real prototype for laboratory study.

The percentage difference in the Mullins effect in Figures 2 and 6 is calculated as being approximately equal to 2.3%, suggesting that the theoretical model can be considered close to the experimental one.

Additionally, there is an opportunity to explore the damping capabilities of the coupling and study the nonlinear characteristics of its behavior in a CAD system by modifying fundamental geometric parameters.

Author Contributions: Conceptualization, S.T. and A.B.; methodology, S.T.; software, S.T.; validation, I.M., S.S. and R.H.; formal analysis, N.N.; investigation, P.N.; resources, P.N.; data curation, S.P.; writing—original draft preparation, S.T.; writing—review and editing, A.A.; visualization, N.N.; supervision, S.T.; project administration, A.A.; funding acquisition, R.H. All authors have read and agreed to the published version of the manuscript.

Funding: This research was funded by the Technical university of Varna, Bulgaria.

Institutional Review Board Statement: Not applicable.

Informed Consent Statement: Not applicable.

Data Availability Statement: Data are contained within the article.

Conflicts of Interest: The authors declare no conflicts of interest.

References

1. Diani, J.; Fayolle, B.; Gilormini, P. A review on the Mullins effect. *Eur. Polym. J.* **2009**, *45*, 601–612. [CrossRef]
2. Cantournet, S.; Desmorat, R.; Besson, J. Mullins effect and cyclic stress softening of filled elastomers by internal sliding and friction thermodynamics model. *Int. J. Solids Struct.* **2009**, *46*, 2255–2264. [CrossRef]
3. St. Rickaby, R.; Scott, N.H. *The Mullins Effect, Constitutive Models for Rubber VII*; Jerrams, S., Murphy, N., Eds.; Taylor & Francis: London, UK, 2011; pp. 273–276. [CrossRef]
4. Fu, W.; Wang, L.; Huang, J.; Liu, C.; Peng, W.; Xiao, H.; Li, S. Mechanical Properties and Mullins Effect in Natural Rubber Reinforced by Grafted Carbon Black. *Adv. Polym. Technol.* **2019**, *2019*, 4523696. [CrossRef]
5. Wang, C.C.; Zhang, Y.F.; Liu, Q.Q.; Wang, Z.B. Mullins Effect under Compression Mode and its Reversibility of Thermoplastic Vulcanizate Based on Ethylene-Vinyl Acetate Copolymer/Styrene-Butadiene Rubber Blend. *Int. Polym. Process.* **2017**, *32*, 11–19. [CrossRef]
6. Stoyanov, S.; Hristov, H.; Tenev, S.; Spasov, N. Determining the damping capability of an elastic coupling with a rubber element type "SEGE". *J. Mech. Eng. Technol.* **2012**, *1*, 61–66.
7. *BDS 16420-86*; Elastic Coupling with Rubber Element. Basic Parameters, Dimensions and Technical Requirements. Bulgarian Institute for Standardization: Sofia, Bulgaria. Available online: https://bds-bg.org/en/ (accessed on 23 July 2024).
8. Kallinikidou, E. Nonlinear Analysis of Plastic and Rubber Components with SolidWorks Simulation. *Doc. Simul. Prod. Dassault Syst.* **2010**, *33*.
9. Steffen, J. *Analysis of Machine Elements Using SolidWorks Simulation 2012*; Schroff Development Corporation: Mission, KS, USA, 2012; p. 390.
10. Shih, R. *Introduction to Finite Element Analysis Using SolidWorks Simulation 2013*; Schroff Development Corporation: Mission, KS, USA, 2012.
11. Kurowski, P.M. *Engineering Analysis with SolidWorks Simulation 2012*; SDC Publications: Mission, KS, USA, 2012.
12. Weber, M. *SolidWorks Simulation 2014 Black Book*; CreateSpace Independent Publishing Platform: Scotts Valley, CA, USA, 2014.
13. Lee, H. *Mechanics of Materials Labs with SolidWorks Simulation 2013*; SDC Publications: Mission, KS, USA, 2013.
14. Pacheco, J.E.L.; Bavastri, C.A.; Pereira, J.T. Viscoelastic Relaxation Modulus Characterization Using Prony Series. *Lat. Am. J. Solids Struct.* **2015**, *12*, 420–445. [CrossRef]
15. Londono, J.G.; Berger-Vergiat, L.; Waisman, H. A Prony-series type viscoelastic solid coupled with a continuum damage law for polar ice modeling. *Mech. Mater.* **2016**, *98*, 81–97. [CrossRef]
16. Sorvari, J. Modelling Methods for Viscoelastic Constitutive Modelling of Paper. Doctoral Dissertation, Department of Physics University of Kuopio, Kuopio, Finland, 2009; p. 115.
17. Botz, M.; Kraus, M.; Siebert, G. *Experimental Determination of the Shear Modulus of Polymeric Interlayers Used in Laminated Glass*; GlassCon Global: Chicago, IL, USA, 2018; p. 8.
18. Sun, Y.; Gu, Z.; Wang, J.; Yuan, X. Research of Method for Solving Relaxation Modulus Based on Three-Point Bending Creep Test. *Materials* **2019**, *12*, 2021. [CrossRef] [PubMed]
19. Tenev, S. *Reducing of Work Rubber Arms Load of an Engine Mount, Mechanics of Machines XXIV*; Technical University of Varna: Varna, Bulgaria, 2021; Volume 1, pp. 22–35.
20. Akin, J. (Ed.) *Finite Element Analysis Concepts via SolidWorks*, 1st ed.; WSPC: Paleo Faliro, Greece, 2010; p. 348.

Disclaimer/Publisher's Note: The statements, opinions and data contained in all publications are solely those of the individual author(s) and contributor(s) and not of MDPI and/or the editor(s). MDPI and/or the editor(s) disclaim responsibility for any injury to people or property resulting from any ideas, methods, instructions or products referred to in the content.